Cavity model of circularly polarised cross-aperture-coupled microstrip antenna

B.Al-Jibouri, H.Evans, E.Korolkiewicz, E.G.Lim, A.Sambell and T.Viasits

Abstract: A cavity model is used to analyse an aperture-fed nearly square circularly polarised patch antenna. The form of the aperture is that of a symmetric cross-slot that couples the excitation between a single microstrip feed line and the patch antenna. Using equivalent magnetic current sources at the slots, the modal electric and magnetic fields under the patch are obtained, and hence analytical expressions for the patch admittances at the aperture are derived and used to obtain an equivalent circuit of the circular polarised antenna. Good agreement is obtained between the circuit modelling and practical results.

1 Introduction

An aperture-coupled feed structure is known to have a number of practical advantages. Since the feed network and radiating patch are on separate substrates, both the thickness and dielectric properties of each substrate can be independently chosen to meet requirements of the feed network to the radiation patch. The isolation of the patch from the feed network by the ground plane minimises spurious feed radiation. A compact structure can be realised using aperture coupling, and as the aperture is positioned below the centre of the patch, the symmetry ensures good circular polarisation [1, 2].

Aperture-coupled structures have been fully analysed using spectral domain [3, 4] and spatial solution [5] methods. These analyses can be used to examine the effects of the design parameters on the performance of the antenna with good accuracy. However, these approaches are numerically intensive and, because of the poor convergence of the reaction integrals and tabulation of Green's functions, can be time consuming and require expensive computations. In addition, these methods of analysis do not produce equivalent circuit models which are suitable for small-scale CAD computations.

Although not as rigorous as the above full-wave analyses, the cavity model [6, 7] can readily be used to derive equivalent circuit models of the antennas for implementation of small-scale CAD. It has been shown that in the cavity model the antenna substrate thickness must be much less than the free-space wavelength [8], a condition normally satisfied in the design of microstrip patch antenna structures.

In this paper the cavity model has been used to model a circularly polarised nearly square patch antenna, excited using a microstrip feed line via a symmetrical cross-slot [1, 2, 9]. In contrast to a single slot structure the cross-slot structure allows the use of slot length greater than half the patch width; hence the matching condition is maintained over a wider bandwidth. In addition, the equal cross slots provide symmetry of excitation of the patch and ensure generation of circular polarisation with good axial ratio [2, 10]. An equivalent circuit model has been derived and used to determine the input impedance of the antenna and further, based on the derived equivalent circuit the conditions for producing a good axial ratio are also examined. It is shown that there is a close agreement between the practical results and those predicted by the cavity model approach.

2 Field distribution

The structure of the antenna using a symmetrical cross-slot is shown in Fig. 1, where it is assumed that the electric field distribution in each of the two orthogonal apertures is in the form of a single piece-wise sinusoidal mode [3]. The electric field in the aperture parallel to the y axis has only an x-directed component E_{ax}, given by

$$E_{ax} = \frac{V_{0y}}{W_a}\frac{\sin\left[k_a\left(\frac{L_a}{2}-\left|y-\frac{b}{2}\right|\right)\right]}{\sin\left(k_a\frac{L_a}{2}\right)} \quad \begin{matrix} \frac{a-W_a}{2} \le x \le \frac{a+W_a}{2} \\ \frac{b-L_a}{2} \le y \le \frac{b-L_a}{2} \\ z = 0 \end{matrix}$$
$$= 0, \qquad \text{otherwise} \tag{1}$$

where V_{0y} is the voltage at the centre of the aperture parallel to the y axis and k_a is the wave number of the aperture determined by Cohn's method [11]. Similarly, the electric field in the aperture parallel to the x axis has only a y component E_{ay} given by

$$E_{ay} = \frac{V_{0x}}{W_a}\frac{\sin\left[k_a\left(\frac{L_a}{2}-\left|x-\frac{b}{2}\right|\right)\right]}{\sin\left(k_a\frac{L_a}{2}\right)} \quad \begin{matrix} \frac{a-L_a}{2} \le x \le \frac{a+L_a}{2} \\ \frac{b-W_a}{2} \le y \le \frac{b-W_a}{2} \\ z = 0 \end{matrix}$$
$$= 0, \qquad \text{otherwise} \tag{2}$$

where V_{0x} is the voltage at the middle of the aperture parallel to the x axis.

IEE Proceedings online no. 20010498

DOI: 10.1049/ip-map:20010498

Paper first received 13th September 2000 and in revised form 23rd April 2001

The authors are with the School of Engineering, University of Northumbria at Newcastle, Ellison Building, Ellison Place, Newcastle upon Tyne, NE1 8ST, UK

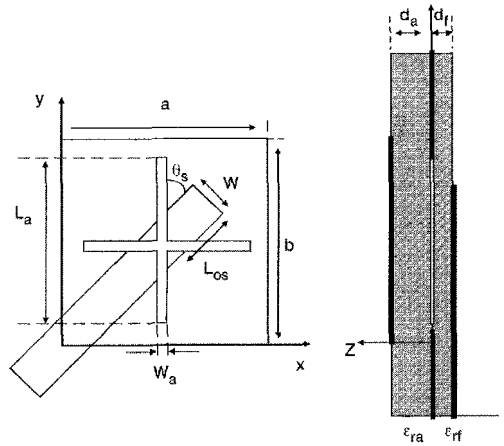

Fig. 1 *Design parameters of cross-aperture coupled microstrip antenna*
$a = 32.1$mm, $b = 34.5$mm, $W = 4.724$mm, $L_{os} = 9$mm, $L_a = 18$mm, $W_a = 2$mm, $\varepsilon_{ra} = 2.33$, $\varepsilon_{rf} = 2.33$, $d_a = 3.15$mm, $d_f = 1.575$mm, $\phi_s = \pm 45°$

The cavity models [12] assumes that the tangential magnetic field at the cavity side walls is zero to a good approximation, and, by the equivalence principle [12], the magnetic currents in each of the two apertures just above the ground plane are then given by

$$M_{ax} = -2E_{ay} \tag{3}$$

and

$$M_{ay} = 2E_{ax} \tag{4}$$

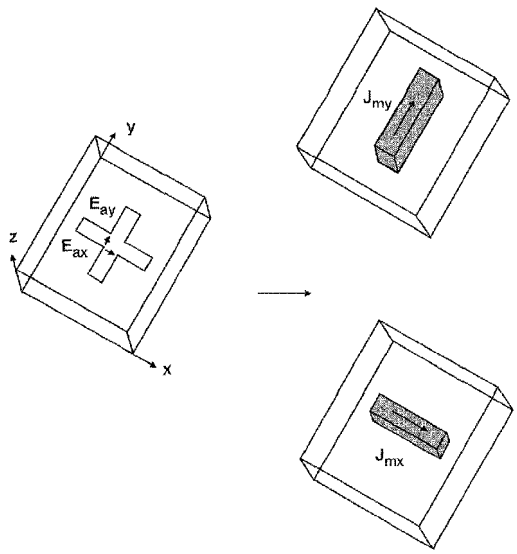

Fig. 2 *Equivalent magnetic currents replacing electric fields in aperture*

The equivalent magnetic current density excitation is assumed to be uniformly distributed in the cavity volume above the slot [13] as shown in Fig. 2. The corresponding current densities J_{mx} and J_{my} in the aperture cavities are therefore given by

$$J_{mx} = \begin{cases} \frac{-2V_{0x}}{d_a W_a} \frac{\sin\left[k_a\left(\frac{L_a}{2} - \left|x - \frac{a}{2}\right|\right)\right]}{\sin\left(k_a \frac{L_a}{2}\right)} & \begin{matrix} \frac{a-L_a}{2} \le x \le \frac{a+L_a}{2} \\ \frac{b-W_a}{2} \le y \le \frac{b+W_a}{2} \\ 0 \le z \le d_a \end{matrix} \\ 0, & \text{otherwise} \end{cases} \tag{5}$$

and

$$J_{my} = \begin{cases} \frac{2V_{0y}}{d_a W_a} \frac{\sin\left[k_a\left(\frac{L_a}{2} - \left|y - \frac{b}{2}\right|\right)\right]}{\sin\left(k_a \frac{L_a}{2}\right)} & \begin{matrix} \frac{a-W_a}{2} \le x \le \frac{a+W_a}{2} \\ \frac{b-L_a}{2} \le y \le \frac{b+L_a}{2} \\ 0 \le z \le d_a \end{matrix} \\ 0, & \text{otherwise} \end{cases} \tag{6}$$

The magnetic field $\boldsymbol{H}$ inside the cavity volume due to the magnetic current density $\boldsymbol{J}_m$ is given by Maxwell's equation

$$\nabla \times \nabla \times \boldsymbol{H} - k^2 \boldsymbol{H} = -j\omega\mu_0 \boldsymbol{J}_m \tag{7}$$

For the magnetic fields $\boldsymbol{H}_x$, $\boldsymbol{H}_y$ which only have x and y components, eqn. 7 reduces to the following two differential equations:

$$\frac{\partial^2 H_y}{\partial x \partial y} - \frac{\partial^2 H_x}{\partial y^2} - k^2 H_x = -j\omega\mu_0 J_{mx} \tag{8}$$

$$\frac{\partial^2 H_x}{\partial x \partial y} - \frac{\partial^2 H_y}{\partial y^2} - k^2 H_y = -j\omega\mu_0 J_{my} \tag{9}$$

The solution of the above differential equations can be expressed in the following eigenfunction expansion form

$$H_x = \sum_m \sum_n B_{x,mn} \Psi_{x,mn} \tag{10}$$

$$H_y = \sum_m \sum_n B_{y,mn} \Psi_{y,mn} \tag{11}$$

where $B_{x,mn}$ and $B_{y,mn}$ are the unknown mode coefficients and $\Psi_{x,mn}$ and $\Psi_{y,mn}$ are the eigenfunction of eqns. 8 and 9. The eigenfunction must satisfy the associated homogenous equations and hence

$$\frac{\partial_2 \Psi_{x,mn}}{\partial x \partial y} - \frac{\partial^2 \Psi_{y,mn}}{\partial y^2} - k_{mn} \Psi_{x,mn} = 0 \tag{12}$$

$$\frac{\partial_2 \Psi_{y,mn}}{\partial x \partial y} - \frac{\partial^2 \Psi_{x,mn}}{\partial y^2} - k_{mn} \Psi_{y,mn} = 0 \tag{13}$$

where k_{mn} are the associated eigenvalues. The boundary conditions on the four magnetic walls are

$$\begin{aligned} \Psi_{x,mn} &= 0 \text{ at } y = 0 \text{ and } y = b \\ \Psi_{y,mn} &= 0 \text{ at } x = 0 \text{ and } x = a \end{aligned} \tag{14}$$

The eigenfunctions are given by

$$\Psi_{x,mn} = A_{mn}.k_n.\cos(k_m x)\sin(k_n y) \tag{15}$$

$$\Psi_{y,mn} = A_{mn}.k_n.\cos(k_n y)\sin(k_m x) \tag{16}$$

with

$$A_{mn} = \sqrt{\frac{\chi_m \chi_n}{ab}}, \text{ where } \chi_p = \begin{cases} 1 & \text{if } p = 0 \\ 2 & \text{if } p \neq 0 \end{cases} \tag{17}$$

and

$$k_m = \frac{m.\pi}{a}, \qquad k_n = \frac{n.\pi}{b} \tag{18}$$

The mode coefficients $B_{x,mn}$ and $B_{y,mn}$ can be found by substituting for H_x and H_y from eqns. 10 and 11 into the non-homogeneous differential eqns. 8 and 9 to give

$$\sum_m \sum_n B_{x,mn}(k_{mn}^2 - k^2)\Psi_{x,mn} = -j\omega\varepsilon J_{mx} \tag{19}$$

and,

$$\sum_m \sum_n B_{y,mn}(k_{mn}^2 - k^2)\Psi_{y,mn} = -j\omega\varepsilon J_{my} \tag{20}$$

Multiplying eqn. 19 with the mode function $\Psi_{x,m'n'}$ and eqn. 20 by $\Psi_{y,m'n'}$ and integrating over the cavity volume of

the patch gives

$$\sum_m \sum_n B_{x,mn}(k_{mn}^2 - k^2) \int_0^a \int_0^b \Psi_{x,mn}\Psi_{x,m'n'}dxdy$$

$$= -j\omega\varepsilon \int_0^a \int_0^b J_{mx}\Psi_{x,m'n'}dxdy \quad (21)$$

and,

$$\sum_m \sum_n B_{y,mn}(k_{mn}^2 - k^2) \int_0^a \int_0^b \Psi_{y,mn}\Psi_{y,m'n'}dxdy$$

$$= -j\omega\varepsilon \int_0^a \int_0^b J_{my}\Psi_{y,m'n'}dxdy \quad (22)$$

The orthogonal properties of $\Psi_{x,mn}$ and $\Psi_{y,mn}$ are

$$\int_0^a \int_0^b \Psi_{x,mn}\Psi_{x,m'n'}dxdy = \begin{cases} k_n^2 & \text{if } m = m' \text{ and } n = n' \\ 0 & \text{otherwise} \end{cases} \quad (23)$$

$$\int_0^a \int_0^b \Psi_{y,mn}\Psi_{y,m'n'}dxdy = \begin{cases} k_m^2 & \text{if } m = m' \text{ and } n = n' \\ 0 & \text{otherwise} \end{cases} \quad (24)$$

hence

$$B_{x,mn} = \frac{j\omega\varepsilon}{(k^2 - k_{mn}^2)\cdot k_n^2} \int_0^a \int_0^b J_{mx}\Psi_{x,mn}dxdy \quad (25)$$

$$B_{y,mn} = \frac{j\omega\varepsilon}{(k^2 - k_{mn}^2)\cdot k_m^2} \int_0^a \int_0^b J_{my}\Psi_{y,mn}dxdy \quad (26)$$

Substituting for J_{mx}, J_{my}, $\Psi_{x,mn}$ and $\Psi_{y,mn}$ integrating eqns. 25 and 26 gives

$$B_{x,mn} = \frac{-j\omega\varepsilon.A_{mn}V_{0x}}{d_a k_n \cdot (k^2 - k_{mn}^2)} \cdot \frac{4\,\mathrm{sinc}\left(k_n\frac{W_a}{2}\right)\sin\left(\frac{n\pi}{2}\right)\cos\left(\frac{m\pi}{2}\right)}{\sin\left(k_a\frac{L_a}{2}\right)} \cdot \frac{k_a\left[\cos\left(k_m\frac{L_a}{2}\right) - \cos\left(k_a\frac{L_a}{2}\right)\right]}{k_a^2 - k_m^2} \quad (27)$$

$$B_{y,mn} = \frac{-j\omega\varepsilon.A_{mn}V_{0y}}{d_a k_m \cdot (k^2 - k_{mn}^2)} \cdot \frac{4\,\mathrm{sinc}\left(k_m\frac{W_a}{2}\right)\sin\left(\frac{m\pi}{2}\right)\cos\left(\frac{n\pi}{2}\right)}{\sin\left(k_a\frac{L_a}{2}\right)} \cdot \frac{k_a\left[\cos\left(k_n\frac{L_a}{2}\right) - \cos\left(k_a\frac{L_a}{2}\right)\right]}{k_a^2 - k_n^2} \quad (28)$$

With the known mode coefficients the components of the magnetic field in the patch cavity are given by

$$H_x = \sum_m \sum_n A_{mn}B_{x,mn}k_n \cos(k_m x)\sin(k_n y) \quad (29)$$

$$H_y = \sum_m \sum_n A_{mn}B_{y,mn}k_m \sin(k_m x)\cos(k_n y) \quad (30)$$

Finally the electric field $\boldsymbol{E}_z$ can be determined from the Maxwell equation

$$E_{z(x,y)} = \frac{1}{j\omega\varepsilon}\left[\frac{dH_y}{dx} - \frac{dH_x}{dy}\right] \quad (31)$$

giving

$$E_{z(x,y)} = \frac{1}{j\omega\varepsilon}\sum_m \sum_n A_{mn}C_{mn}\cos(k_m x)\cos(k_n y) \quad (32)$$

where

$$C_{mn} = B_{x,mn}k_m^2 - B_{y,mn}k_n^2 \quad (33)$$

Hence, the electromagnetic fields in the volume of the patch are now known and defined by eqns. 29, 30 and 32. The losses in the cavity can also be taken into account by replacing k by an effective wave number [5]

$$k_{eff}^2 = k_0^2\varepsilon_r(1 - j\delta_{eff}) \quad (34)$$

where δ_{eff} is the effective loss tangent, which includes the radiation and copper dielectric losses [14].

3 Input impedance

The admittances of the patch of the two orthogonal apertures can be evaluated using the energy conservation theorem [12] and are given by

$$Y_{x,ant} = \frac{\iiint_V H_x J_{mx}^* dv}{|V_{0x}|^2} \quad \text{and } Y_{y,ant} = \frac{\iiint_V H_y J_{my}^* dv}{|V_{0y}|^2} \quad (35)$$

Substituting the expression for the magnetic field from eqns. 29 and 30 and the magnetic current density from eqns. 5 and 6, and performing the integration, the following analytical formulas are obtained for the admittance values of the antenna at the apertures:

$$Y_{x,ant} = \sum_m \sum_n \frac{16\cdot j\omega\varepsilon\cdot A_{mn}^2}{d_a\left((k^*)^2 - k_{mn}^2\right)} \cdot \left\{\frac{\mathrm{sinc}\left(k_n\frac{W_a}{2}\right)\sin\left(\frac{n\pi}{2}\right)\cos\left(\frac{m\pi}{2}\right)}{\sin\left(k_a\frac{L_a}{2}\right)} \cdot \frac{k_a\left[\cos\left(k_m\frac{L_a}{2}\right) - cos\left(k_a\frac{L_a}{2}\right)\right]}{k_a^2 - k_m^2}\right\}^2 \quad (36)$$

$$Y_{y,ant} = \sum_m \sum_n \frac{16\cdot j\omega\varepsilon\cdot A_{mn}^2}{d_a\left((k^*)^2 - k_{mn}^2\right)} \cdot \left\{\frac{\mathrm{sinc}\left(k_m\frac{W_a}{2}\right)\sin\left(\frac{m\pi}{2}\right)\cos\left(\frac{n\pi}{2}\right)}{\sin\left(k_a\frac{L_a}{2}\right)} \cdot \frac{k_a\left[\cos\left(k_n\frac{L_a}{2}\right) - cos\left(k_a\frac{L_a}{2}\right)\right]}{k_a^2 - k_n^2}\right\}^2 \quad (37)$$

The self-admittance of the aperture is obtained by considering it as two short-circuited slot lines of length $L_a/2$, and, is thus given by

$$Y_{ap} = -\frac{2j}{Z_{ca}} \cot\left(k_a \frac{L_a}{2}\right) \tag{38}$$

Finally, the input impedance of the antenna is given by the following expression:

$$Z_{in} = \frac{n^2}{Y_{x,ant} + Y_{ap}} + \frac{n^2}{Y_{y,ant} + Y_{ap}} - jZ_f \cot(k_f L_{os}) \tag{39}$$

where n is the turns ratio of the microstrip to aperture impedance transformation for the two orthogonal apertures, k_f is the wave number of the feed line [10, 13].

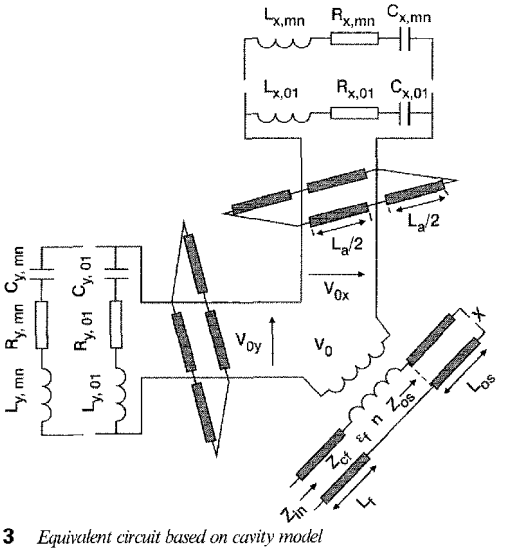

Fig. 3 *Equivalent circuit based on cavity model*

4 Equivalent circuit

Using the developed analytic expressions (see eqns. 36 and 37) for the patch admittances at the apertures, it is possible to draw an equivalent circuit of the cross-aperture coupled CP antenna based on the cavity method as shown in Fig. 3. Eqns. 36 and 37 can be written in the form

$$Y_{x,ant} = \sum_m \sum_n \frac{16 \cdot j\omega\varepsilon \cdot A_{mn}^2}{d_a[\omega^2 - \omega_{mn}^2]\left(1 + j\delta_{eff}\frac{\omega^2}{\omega_{mn}^2}\right)} \cdot \left\{ \frac{\operatorname{sinc}\left(k_n \frac{W_a}{2}\right) \sin\left(\frac{n\pi}{2}\right) \cos\left(\frac{m\pi}{2}\right)}{\sin\left(k_a \frac{L_a}{2}\right)} \cdot \frac{k_a\left[\cos\left(k_m \frac{L_a}{2}\right) - \cos\left(k_a \frac{L_a}{2}\right)\right]}{k_a^2 - k_m^2} \right\}^2 \tag{40}$$

$$Y_{y,ant} = \sum_m \sum_n \frac{16 \cdot j\omega\varepsilon \cdot A_{mn}^2}{d_a[\omega^2 - \omega_{mn}^2]\left(1 + j\delta_{eff}\frac{\omega^2}{\omega_{mn}^2}\right)} \cdot \left\{ \frac{\operatorname{sinc}\left(k_m \frac{W_a}{2}\right) \sin\left(\frac{m\pi}{2}\right) \cos\left(\frac{n\pi}{2}\right)}{\sin\left(k_a \frac{L_a}{2}\right)} \cdot \frac{k_a\left[\cos\left(k_n \frac{L_a}{2}\right) - \cos\left(k_a \frac{L_a}{2}\right)\right]}{k_a^2 - k_n^2} \right\}^2 \tag{41}$$

Each of these formulas corresponds to the expression of the admittance of $m \times n$ series RCL circuits, which are all connected in parallel (see Fig. 3). The equivalent circuit of the patch admittance, as seen by the slot parallel to the y axis, have the following circuit elements:

$$L_{x,mn} = \frac{d_a}{16\varepsilon c^2 A_{mn}^2} \cdot \left\{ \frac{\operatorname{sinc}\left(k_n \frac{W_a}{2}\right) \sin\left(\frac{n\pi}{2}\right) \cos\left(\frac{m\pi}{2}\right)}{\sin\left(k_a \frac{L_a}{2}\right)} \cdot \frac{k_a\left[\cos\left(k_m \frac{L_a}{2}\right) - \cos\left(k_a \frac{L_a}{2}\right)\right]}{k_a^2 - k_m^2} \right\}^2$$

$$C_{x,mn} = L_{x,mn}^{-1} \frac{\varepsilon_{ra} k_{mn}^2}{c^2} \qquad R_{x,mn} = L_{x,mn} k_{mn} c \delta_{eff} \tag{42}$$

Similarly, the equivalent circuit of the patch, as seen by the slot parallel to the x axis, have circuit elements:

$$L_{y,mn} = \frac{d_a}{16\varepsilon c^2 A_{mn}^2} \cdot \left\{ \frac{\operatorname{sinc}\left(k_m \frac{W_a}{2}\right) \sin\left(\frac{m\pi}{2}\right) \cos\left(\frac{n\pi}{2}\right)}{\sin\left(k_a \frac{L_a}{2}\right)} \cdot \frac{k_a\left[\cos\left(k_n \frac{L_a}{2}\right) - \cos\left(k_a \frac{L_a}{2}\right)\right]}{k_a^2 - k_n^2} \right\}^2$$

$$C_{y,mn} = L_{y,mn}^{-1} \frac{\varepsilon_{ra} k_{mn}^2}{c^2} \qquad R_{y,mn} = L_{y,mn} k_{mn} c \delta_{eff} \tag{43}$$

5 Axial ratio

For the calculation of the axial ratio, the far field components of the antenna are first determined in the boresight. This is performed by replacing the electrical field at the edges of the patch by equivalent magnetic currents as given by [15]

$$\boldsymbol{M} = 2d_a \cdot E_{z(x,y)} \cdot \boldsymbol{z} \times \boldsymbol{n} \tag{44}$$

where $\boldsymbol{n}$ is the outward normal unit vector to the magnetic wall at the edges of the patch. Substituting the expression of the electric field from eqn. 32 gives the following values of magnetic currents at the four edges of the patch:

$$M_{x(x,y=0)} = \frac{d_a}{j\omega\varepsilon} \sum_m \sum_n A_{mn} C_{mn} \cos(k_m x) \tag{45}$$

$$M_{x(x,y=b)} = -\frac{d_a}{j\omega\varepsilon} \sum_m \sum_n A_{mn} C_{mn} \cos(k_m x) \cdot (-1)^n \tag{46}$$

$$M_{y(x=0,y)} = \frac{d_a}{j\omega\varepsilon} \sum_m \sum_n A_{mn} C_{mn} \cos(k_n y) \tag{47}$$

$$M_{y(x=a,y)} = -\frac{d_a}{j\omega\varepsilon} \sum_m \sum_n A_{mn} C_{mn} \cos(k_n y) \cdot (-1)^m \tag{48}$$

The electrical field $\boldsymbol{E(r)}$ caused by an infinitesimally small magnetic current element ($\boldsymbol{dM}$) is obtained as

$$\boldsymbol{E}(\boldsymbol{r}) = \frac{jk_0 e^{-jk_0 r}}{4\pi r} \cdot \boldsymbol{r} \times d\boldsymbol{M} \tag{49}$$

where $\boldsymbol{r}$ is the unit vector pointing from the magnetic current element to the observation point and r is the distance between the magnetic current and the observation point. The electric field radiated by the patch is obtained by integrating eqn. 49 along the edges of the patch. In the boresight, the components of the electric field are, therefore, given by

$$E_x = \frac{d_a k_0 e^{-jk_0 r}}{4\pi\omega\varepsilon r} \cdot \int_0^b \left(\sum_m \sum_n A_{mn} C_{mn} \cos(k_n y) \cdot (-1)^m - \sum_m \sum_n A_{mn} C_{mn} \cos(k_n y) \right) dy \tag{50}$$

$$E_y = \frac{d_a k_0 e^{-jk_0 r}}{4\pi\omega\varepsilon r} \cdot \int_0^a \left(\sum_m \sum_n A_{mn} C_{mn} \cos(k_m y) - \sum_m \sum_n A_{mn} C_{mn} \cos(k_m y) \cdot (-1)^n \right) dx \tag{51}$$

which simplify to

$$E_x = \frac{d_a k_0 e^{-jk_0 r}}{4\pi\omega\varepsilon r} \cdot \sum_m \sum_n A_{mn} C_{mn} \cdot [(-1)^m - 1] \tag{52}$$

$$E_y = \frac{d_a k_0 e^{-jk_0 r}}{4\pi\omega\varepsilon r} \cdot \sum_m \sum_n A_{mn} C_{mn} \cdot [1 - (-1)^n] \tag{53}$$

where,

$$C_{m0} = \begin{cases} -B_{y,m0} & \text{if } m \text{ odd} \\ 0 & \text{if } m \text{ even} \end{cases} \tag{54}$$

$$C_{0n} = \begin{cases} B_{x,0n} & \text{if } n \text{ odd} \\ 0 & \text{if } n \text{ even} \end{cases} \tag{55}$$

Therefore

$$E_x = \frac{d_a k_0 e^{-jk_0 r}}{4\pi\omega\varepsilon r} \cdot \sum_m A_{m0} B_{y,m0} \tag{56}$$

$$E_y = \frac{d_a k_0 e^{-jk_0 r}}{4\pi\omega\varepsilon r} \cdot \sum_n A_{0n} B_{x,0n} \tag{57}$$

The expressions for $B_{x,0n}$ and $B_{y,m0}$ can be written in the following form:

$$B_{x,0n} = V_{0x} \cdot B'_{x,0n} \tag{58}$$

$$B_{y,m0} = V_{0y} \cdot B'_{y,m0} \tag{59}$$

where

$$B'_{x,0n} = \frac{j\omega\varepsilon . A_{m0}}{d_a k_n \cdot (k^2 - k_n^2)} \cdot \frac{4\,\mathrm{sinc}\left(k_n \frac{W_a}{2}\right) \sin\left(\frac{n\pi}{2}\right)}{\sin\left(k_a \frac{L_a}{2}\right)} \cdot \frac{k_a \left[1 - \cos\left(k_a \frac{L_a}{2}\right)\right]}{k_a^2} \tag{60}$$

$$B'_{y,m0} = \frac{j\omega\varepsilon . A_{0n}}{d_a k_n \cdot (k^2 - k_m^2)} \cdot \frac{4\,\mathrm{sinc}\left(k_m \frac{W_a}{2}\right) \sin\left(\frac{m\pi}{2}\right)}{\sin\left(k_a \frac{L_a}{2}\right)} \cdot \frac{k_a \left[1 - \cos\left(k_a \frac{L_a}{2}\right)\right]}{k_a^2} \tag{61}$$

From the equivalent circuit, the voltages V_{0x} and V_{0y} can be expressed as

$$V_{0x} = V_0 \cdot \frac{(Y_{x,ant} + Y_{ap})^{-1}}{(Y_{x,ant} + Y_{ap})^{-1} + (Y_{y,ant} + Y_{ap})^{-1}} \tag{62}$$

$$V_{0y} = V_0 \cdot \frac{(Y_{y,ant} + Y_{ap})^{-1}}{(Y_{x,ant} + Y_{ap})^{-1} + (Y_{y,ant} + Y_{ap})^{-1}} \tag{63}$$

Substituting these results into the expressions for the electric field components in the boresight gives the computational formulas for the field components E_x and E_y

$$E_x = \frac{V_0 d_a k_0 e^{-jk_0 r}}{2\pi\omega\varepsilon r} \cdot \frac{(Y_{x,ant} + Y_{ap})^{-1}}{(Y_{x,ant} + Y_{ap})^{-1} + (Y_{y,ant} + Y_{ap})^{-1}} \cdot \sum A_{m0} B'_{y,m0} \tag{64}$$

and

$$E_y = \frac{V_0 d_a k_0 e^{-jk_0 r}}{2\pi\omega\varepsilon r} \cdot \frac{(Y_{y,ant} + Y_{ap})^{-1}}{(Y_{x,ant} + Y_{ap})^{-1} + (Y_{y,ant} + Y_{ap})^{-1}} \cdot \sum A_{0n} B'_{x,0n} \tag{65}$$

The amplitude error (Ae) and phase error (ϕ_e) required for the calculation of the axial ratio can be expressed as

$$A_e = \frac{|E_x|}{|E_y|} = \frac{|Y_{y,ant} + Y_{ap}|}{|Y_{x,ant} + Y_{ap}|} \cdot \frac{\left|\sum_m A_{m0} B'_{y,m0}\right|}{\left|\sum_n A_{0n} B'_{x,0n}\right|} \tag{66}$$

$$\phi_e = \angle\left(\frac{E_x}{E_y}\right) = \angle\left(\frac{Y_{y,ant} + Y_{ap}}{Y_{x,ant} + Y_{ap}} \cdot \frac{\sum_m A_{m0} B'_{y,m0}}{\sum_n A_{0n} B'_{x,0n}}\right) \tag{67}$$

Finally, the value of axial ratio is calculated by [12]

$$AR = \sqrt{\frac{1 + A_e^2 + [1 + A_e^4 + 2A_e^2 \cos(2\phi_e)]^{1/2}}{1 + A_e^2 - [1 + A_e^4 + 2A_e^2 \cos(2\phi_e)]^{1/2}}} \tag{68}$$

Eqns. 66 and 67, based on the resonant cavity model, provide a numerical means of determining the axial ratio of the cross-aperture coupled patch antenna at a given frequency when the design parameters shown in Fig. 1 are known.

6 Comparison of cavity method, full wave simulation and experimental results

The input impedance of the antenna with the dimensions in Fig. 1 has been calculated over a frequency range of 2.25–2.7GHz. It can be seen from Fig. 4 that the comparison for the input impedance between cavity model, full wave simulation Ensemble® [16] and experimental results are in good agreement. The impedance loci with the double resonance loop corresponding to the orthogonal modes also demonstrates that good circular polarisation has been achieved. Calculated resonant frequency from the cavity

model of 2.45 GHz is in close agreement with that obtained experimentally and from full-wave simulation.

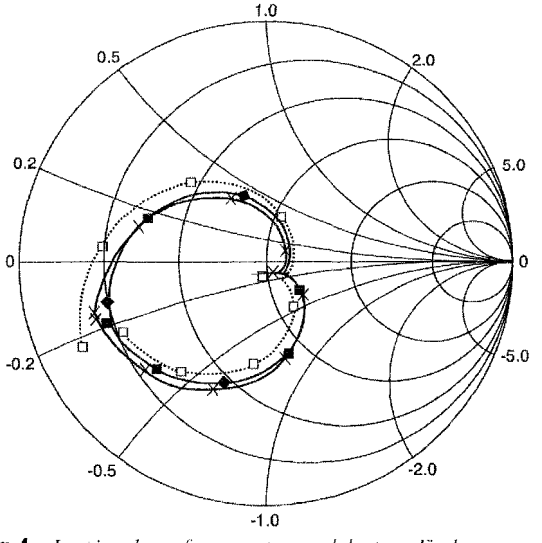

Fig. 4 *Input impedance of cross-aperture coupled antenna Fig. 1*
cavity model
full-wave simulation
experimental results

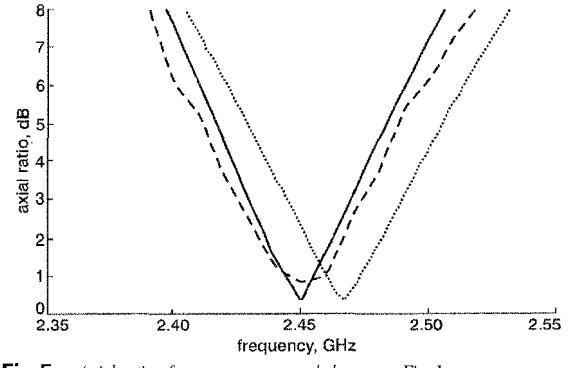

Fig. 5 *Axial ratio of cross-aperture coupled antenna Fig. 1*
cavity model
full-wave simulation
experimental results

The axial ratio (see Fig. 5) has also been evaluated using the cavity model, simulated using Ensemble and practically measured. The prediction of the frequency for the best axial ratio is accurate to about 2% while that prediction of the axial ratio bandwidth is within the range of 10%, when compared with experimental results.

7 Conclusions

Based on the cavity model of the equal cross-slots structure, this paper has presented a theoretical analysis to determine the modal fields under the patch antenna. Using these fields an equivalent circuit of the antenna has been derived which is then used to determine the input impedance and the axial ratio of the circular polarised antenna. This cavity model has been used successfully to design a circular polarised impedance matched antenna. The results based on the cavity model show a good agreement with full-wave simulation and practical results.

8 References

1 POZAR, D.M.: 'Microstrip antenna Aaperture coupled to a microstrip line', *Electron. Lett.*, 1985, **21**, (2), pp. 49–50
2 TARGONSKI, S.D., and POZAR, D.M.: 'Design of widband circularly polarised aperture-coupled microstrip antennas', *IEEE Trans. Antennas Propag.*, 1993, **41**, (2), pp. 214–220
3 SULLIVAN, P.L., and SCHAUBERT, D.H.: 'Analysis of an aperture coupling microstrip antenna', *IEEE Trans. Antennas Propag.*, 1986, **AP-34**, pp. 977–984
4 POZAR, D.M.: 'A reciprocity method of analysis for printed slot and slot-coupled microstrip antennas', *IEEE Trans. Antennas Propag.*, 1986, **AP-34**, (12), pp. 1439–1446
5 BARLATELY, L., SMITH, H.K., and MOSIG, J.R.: 'Printed radiating structures and transitions in multilayered substrates', *Int. J. Microw. Milimeter-Wave Computer-Aided Engineering*, 1992, **2**, pp. 273–285
6 LO, Y.T., ENGST, B., and LEE, R.Q.: 'Simple design formulas for circularly polarised microstrip antennas', *IEE. Proc.-H*, 1988, **135**, pp. 213–215
7 AKSON, M.I., and CHUANG, S.L.: 'On slot-coupled microstrip antennas and their applications to CP operation-theory and experiment', *IEEE Trans. Antennas Propag.*, 1990, **AP-38**, (8), pp. 1224–1230
8 RICHARDS, W.F., LO, Y.T., and HARRISON, D.D.: 'An improved theory for microstrip antennas and applications', *IEEE Trans. Antennas Propag.*, 1981, **AP-29**, pp. 38–46
9 TASO, C.H., HWANG, Y.M., KILLBURG, F., and DIETRICH, F.: 'Aperture-coupled patch antennas with wide-bandwidth and dual polarisation capabilities', *IEEE Antennas Propag. Symp. Dig.*, 1988, pp. 936–939
10 ALJIBOURI, B., VLASITS, T., KOROLKIEWICZ, E., SCOTT, S., and SAMBELL, A.: 'Transmission line modelling of the crossaperture-coupled circular polarised microstrip patch antenn', *IEE Proc. Microw., Antennas Propag.*, 2000, **147**, (2), pp. 82–86
11 CHON, S.B.: 'Slot line on a dielectric substrate', *IEEE Trans. Microw. Theory Techn.*, 1969, **17**, (10), pp. 786–778
12 BALAINS, C.A.: 'Antenna theory: analysis and design' (Wiley & sons, 1989)
13 HIMDI, M., DANIEL, J.P., and TERRENT, C.: 'Analysis of aperture-coupled microstrip antenna using cavity method', *Electron. Lett.*, 1991, **27**, (5), pp. 455–457
14 THOUROUDDE, D., HIMDI, M., and DANIEL, J.P.: 'Cad-oriented cavity model for rectangular patches', *Electron. Lett.*, 1990, **26**, (13), pp. 842–844
15 CARVER, K.R, and MINK, J.W.: 'Microstrip antenna technolog', *IEEE Trans. Antennas Propag.*, 1981, **AP-29**, (1), pp. 2–24
16 ANSOFT Corporation, Ensemble 5.1, 1998